JOURNAL OF MATERIALS SCIENCE 27 (1992) 5911–5915

Local structure of β′-sialons: an EXAFS study study

J. SJÖBERG*, T. ERICSSON‡, O. LINDQVIST
Department of Inorganic Chemistry, Chalmers University of Technology and University of Göteborg, S-41296 Göteborg, Sweden

The local environments of aluminium and silicon in β′-sialons, $Si_{6-z}Al_zN_{8-z}O_z$, have been studied by extended X-ray absorption fine structure spectroscopy. The silicon and aluminium atoms are always in tetrahedral coordination and the refined average bond length between two atomic positions becomes a measure of the distribution of nitrogen and oxygen over the nearest neighbour positions to the absorbing atom. Two β′-sialons samples with different composition, $z = 1$ and $z = 2.7$, were used in the study with α-Si_3N_4, SiO_2 (cristobalite, albite and a xerogel), zeolite NaA, anorthite and AlN as reference substances. The calculated distances to the first coordination sphere for silicon were 0.169 nm for $z = 1$ and 0.168 nm for $z = 2.7$, compared to 0.171 nm for Si_3N_4 under the same conditions. In the aluminium environment, the calculated distances were 0.177 nm for $z = 1$ and 0.176 nm for $z = 2.7$. The results indicate that the β′-sialons are built up by aluminium- and silicon-containing tetrahedra with mixed oxygen and nitrogen environments, although there seems to be a stronger tendency for the formation of Si–N and Al–O bonds, compared to Si–O and Al–N bonds. The results are not precise enough to allow calculation of the contribution from different bond types to the observed average bond lengths; in particular this is due to the short (< 200 eV) Al*K* edge available for structural studies of the β′-sialons.

1. Introduction

Many important properties of sialon materials, e.g. mechanical strength and chemical inertness, reflect the crystal structure of the phases involved [1, 2]. The phase relationships and crystal structures in the system Si_3N_4–AlN–Al_2O_3–SiO_2 are also of general chemical interest. The detailed structure of many of the phases, especially those with varying stoichiometry, have remained unclear, despite several structural studies [3]. Average structures have been obtained by X-ray diffraction [4–6], while ordering phenomena are reported from neutron diffraction work [7, 8]. The local environments around silicon, aluminium and nitrogen atoms have been studied by solid state magic angle spinning nuclear magnetic resonance (MAS NMR) [9–12]. From NMR it would also, ideally, be possible to calculate the fraction of silicon and aluminium atoms in different building units, such as SiN_4, and $SiON_3$, in the various sialon samples. However, the data available from ^{29}Si and ^{15}N NMR studies are obscured by the isomorphous substitution observed for *o*′- and β′-sialons, throughout each region of solid solubility [10–12], while the resolution of the ^{27}Al NMR spectra in most cases is poor, due to severe line broadening caused by second-order quadrupolar interactions [13].

An alternative method in the study of local environments in solids is offered by the extended X-ray absorption fine structure, referred to as EXAFS [14], which is the modulation in the X-ray absorption coefficient, starting somewhat past an absorption edge of the atom of interest. It depends on the interaction between out-going waves of the emitted photoelectron and the waves backscattered from the surrounding atoms. It can be expressed as [15]

$$\chi(k) = \sum_j \frac{N_j F_j(k)}{k R_j^2} e^{-2k^2\sigma_j^2} e^{-2R_j/\lambda} \times \sin[2kR_j + \delta_j(k)] \quad (1)$$

The sum is taken over the coordination shells with radius R_j that contain N_j atoms. The variance in R_j is given by σ_j^2, F_j is the backscattering amplitude and δ_j is the phase shift which depends on the potentials of the central atom and the backscattering atoms. The R_j^{-2} dependence of the magnitude of the contribution from shell j to the EXAFS makes the technique sensitive only to local atomic arrangements. The backscattering amplitudes and the phase shifts can be determined either from model substances or by theoretical calculations, and the EXAFS data can thus be used to determine coordination number, average radius for a shell and σ_j^2 by refining these parameters in a curve-fitting procedure. The refinement can be made on the EXAFS or on its Fourier transform, the pseudo radial distribution function [16].

* Author to whom all correspondence should be addressed.
‡ *Present address*: Experiments Division, ESRF, BP 220, F-38043 Grenoble, France.

© *1992 Chapman & Hall*

The study of variations in bond distances in crystalline phases with known structure but unknown distribution of atoms over possible sites reduces the problem as the coordination number can be fixed [17]. The phases studied must show a considerable range of composition and bond lengths as the precision in the analysis of the EXAFS is measured in thousandths of nanometres [18]. For the sialon system, the requirements are met by the β′-sialons, $Si_{6-z}Al_zN_{8-z}O_z$, which cover a large compositional range ($0 < z < 4$) [5], and has known crystal structure with only one kind of local environment for each atom. EXAFS can be performed on the aluminium and silicon *K* edges; the former is likely to give poor precision due to the interference of the silicon edge only some 200 eV past the aluminium edge. In order to avoid reduction of intensity of the X-radiation through absorption in the guide tubes, EXAFS measurements for the low-energy X-radiation (soft X-rays) required in the study of light atoms (e.g. aluminium and silicon) are carried out under vacuum. Electron-yield detectors are, under these conditions, usually more efficient than photon detectors [19], but electron-yield detection is more surface sensitive. Care must thus be taken to eliminate or estimate the possible influence on the EXAFS from the surface layer, which may differ from the bulk.

In this work the average bond lengths from aluminium and silicon to atoms in the nearest coordination sphere in β′-sialons are measured and compared to reference substances, in particular to α-Si_3N_4, which has a local structure around silicon very similar to that of the β′-sialons. The question addressed is whether silicon in sialons is exclusively surrounded by nitrogen as suggested by NMR work [9], or if there is a substantial number of Si–O bonds. Conclusions drawn from the studies on the β′-sialons are considered to be partly transferable to other phases in the system.

2. Experimental procedure

2.1. Materials

Two β′-sialons, $z = 1.0$ and $z = 2.7$, referred to as B1 and B2, respectively, were used in this study. They were fabricated by AB Sandvik Hard Materials by hot isostatic pressing at 2023 K under a nitrogen pressure of 10 MPa for 2 h, using the glass encapsulation technique. The products were essentially single-phase materials with very little glassy phase [20], although sample B2 contained minute amounts of the sialon polytypoid 15R ($SiAl_4N_4O_2$). Several reference samples were used to compare the EXAFS results with diffraction data. The reference for Si–N bonds was α-Si_3N_4 (SN-E-10), for Si–O bonds it was cristobalite, zeolite NaA and an amorphous silica xerogel. The requirements for the aluminium reference samples were (a) tetrahedral coordination of atoms in the first coordination shell, and (b) ordered structures with respect to Si/Al distribution. Thus, the reference chosen for Al–N bonds was AlN and for Al–O bonds, zeolite NaA and anorthite. As a test sample for mixed composition in the first coordination sphere, Si_2N_2O was used. Samples B1 and B2, as well as the mineral reference materials and the Si_2N_2O were received in pieces and crushed to powder in a cast iron vibrational crush. The Si_2N_2O sample was etched in 2M NaOH solution and aqua regia to remove the glassy phase and metal impurities present.

2.2. Characterization of the samples

Because the Auger detection technique is surface sensitive (penetration depth for aluminium is about 13 nm [21], and expected to be somewhat deeper for silicon [19]), the contributions from the non-representative oxide scale of the nitrogen-containing samples had to be evaluated. The surface layer of sample B1 and the α-Si_3N_4 reference were studied by transmission electron microscopy in a Jeol 2000FX instrument. Powder grains of the samples were deposited on a holey carbon film where individual grains could be observed. In addition to this investigation, product information of the commercial powders were used to estimate the oxide scale thickness. In addition, the specific surface area of AlN was measured by the BET method with nitrogen as adsorbate.

2.3. The EXAFS experiments and analysis

The EXAFS data were acquired on the SOXAFS (soft EXAFS) station at the Synchrotron Radiation Source at the Daresbury Laboratory, UK (station 3.4). The samples were mixed with graphite* and acetone to a slurry which was applied to flat surface holders of stainless steel. The holders were mounted with the flat surface perpendicular to the incoming beam. Radiation monochromatized by quartz crystals was used for the experiments on the aluminium *K* edge, while an InSb monochromator was used for the silicon *K* edge. To allow the low-energy radiation required for the aluminium absorption edge to be reflected in the glancing incidence mirror, the geometry of the experimental apparatus had to be changed, so the focal point of the beam was moved some 4 m from the sample chamber with loss of intensity as a consequence. The intensity was monitored before, I_0, and after, I_{in}, the monochromator and the absorption was measured by total Auger yield, I_{sig}. The EXAFS is then given by I_{in}/I_{sig} [22]. The whole experimental environment (glancing incidence mirror, beam guide, monochromator and sample chamber) was kept under vacuum ($< 10^{-4}$ Pa) during acquisition.

The software operating the spectrometer also included routines for data reduction. The maximum of the derivative of the absorption curve was taken as the position of the edge. The pre-edge background was defined by a linear function while a single third-order polynomial was fit to the post-edge background in a graphics interactive mode. The resulting background subtracted EXAFS was Fourier transformed, filtered and back transformed. The refinements were carried

* For Si*K* edge samples: Goodfellow < 0.5 mm, 99.999%; For Al*K* edge samples: BDH Chemicals Ltd. Synthetic graphite.

out in k-space with k^3 weights applied with the program EXCURV90 which uses a spherical wave algorithm [23]. It uses phase shifts and backscattering amplitudes calculated by the program MUFPOT [24] with "$Z + 1$ 1 s core hole" approximation for the central atom with data on atomic potentials extracted from the Daresbury data base [25]. The statistical validity of the calculated shells was assessed by published means [26]. Background subtraction, Fourier transform and Fourier filtering were carried out in a uniform manner for all samples. The refinements included absorption edge position, E_0, radii of the coordination spheres, R_j, and corresponding variances, σ_j^2. Two spheres were used in refinements where overlap in the Fourier transform of the EXAFS prevented them to be effectively separated in the filtering step; in other cases, only the first shell was used. Coordination numbers of aluminium and silicon were fixed to 4.

3. Results and discussion

The measured specific surface area for the AlN reference was 1.1 $m^2 g^{-1}$, while the value reported for the α-Si_3N_4 powder is 10 $m^2 g^{-1}$ [27]. For AlN with approximately 2.5 wt % oxygen, the oxide surface layer can be estimated to tenths of nanometres, which might severely affect the EXAFS measurements. For Si_3N_4 powders, on the other hand, the high surface area and a reported oxygen content of 2 wt % [27] indicates an oxide scale of about 2 nm. In the electron micrographs of the α-Si_3N_4 powder the oxide scale is indeed seen to be approximately 2 nm, Fig. 1a. The oxide in the β'-sialon samples is found in the thin intergranular phase which for sample B1 is about 2 nm, Fig. 1b. It is thus concluded that the influence of the surface oxide scale on the EXAFS is limited and similar in the reference α-Si_3N_4 and the β'-sialons, while EXAFS measurements on the AlN reference samples using Auger detection may be influenced by the thick surface oxide.

The fit of the calculated EXAFS and its Fourier transform to the experimental data are shown in Fig. 2 for sample B2 and in Fig. 3 for the α-Si_3N_4 reference. The results from the EXAFS measurements are summarized in Table I, which also includes literature values for the reference samples of bond lengths determined from diffraction studies. The statistical errors for the bond lengths in the first coordination sphere were invariably well below 0.001 nm for the SiK edge and ≈ 0.002 nm for the AlK edge. The bond lengths determined from EXAFS analysis for the reference samples are in good agreement with diffraction data, except for AlN. This deviation may have several causes: the oxide scale is thick enough to considerably influence the EXAFS of AlN; the potentials used for aluminium and nitrogen in the calculations might not be entirely satisfactory for this specific atomic configuration [26]; the precision in bond length determination from EXAFS on the AlK edge is poor due to the limited edge available. In addition, the bond lengths

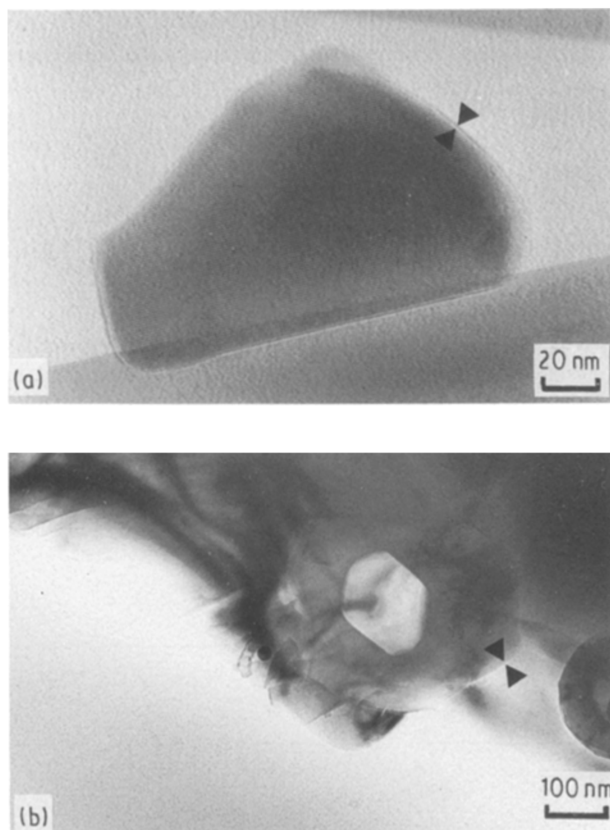

Figure 1 TEM bright-field images showing thin amorphous films (≈ 2 nm) on the surfaces of powder particles. (a) Lattice fringe image of an Si_3N_4 powder particle where an amorphous film (arrowed) can be seen surrounding the particle; (b) a triple grain junction in ground B1 material showing the thin amorphous film (arrowed) to be continuous between the grains.

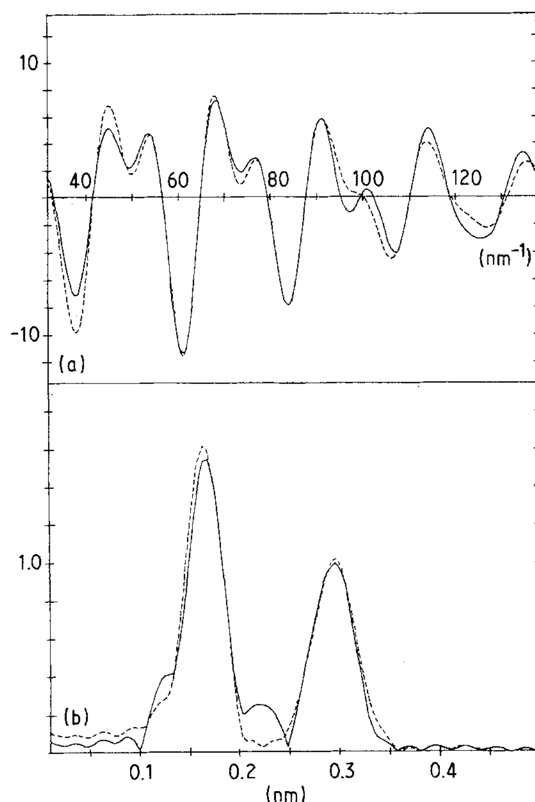

Figure 2 (a) Contribution to SiK edge $k^3\chi(k)$ from the first and second scales in sample B2, and (b) its radial distribution function; (———) experimental and (– – –) theoretical.

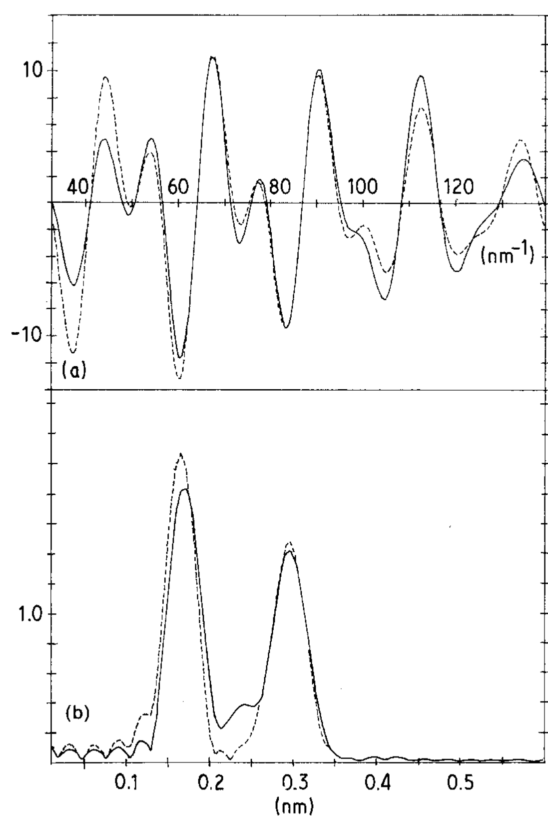

Figure 3 (a) Contribution to Si*K* edge $k^3\chi(k)$ from the first and second scales in α-Si_3N_4, and (b) its radial distribution function; (———) experimental and (- - -) theoretical.

determined by EXAFS have been considered to become generally somewhat too short [34].

The difference in Si–N bond lengths observed for α-Si_3N_4 and sample B2 is 0.003 nm, compared to the expected difference of 0.004 nm for totally random distribution of nitrogen and oxygen with respect to aluminium and silicon in sample B2. In the calculations of mean distances for the first and second coordination spheres of silicon, comparison is made between samples (B1, B2 and α-Si_3N_4) which are structurally very similar, and errors other than the statistical ones should be of similar magnitude, especially because surface effects have been concluded to be small. In the model used for refinements on the silicon data for samples B1, B2 and α-Si_3N_4, the first shell contains only nitrogen and the second only silicon. In β′-sialons, oxygen and aluminium may have replaced nitrogen and silicon, but using these elements to calculate potentials would only further shorten the calculated mean bond lengths of the first coordination sphere of silicon by less than 0.001 nm, thus slightly increasing the difference to that of α-Si_3N_4. The procedure used is preferred, because it enables reliable comparison to be made between samples. In a similar way, the refinement in the aluminium *K* edge case oxygen atoms were used for the first coordination sphere and silicon in the second coordination sphere in the refined model to make it similar to the AlO_4 reference materials used. The differences observed for the Al–O distances are compatible with those determined for the silicon atoms but, as discussed above, the precision in the calculation is poor for the aluminium *K* edge, Fig. 4.

The observed shortening of the bond lengths around silicon in the β′-sialons as compared to Si_3N_4 makes a proposed β′-sialon structure unlikely where silicon is only found in SiN_4 units. Rather, the results support the view that tetrahedral environments around silicon atoms include both oxygen and nitrogen in β′-sialons, possibly with a preference for aluminium to coordinate oxygen and silicon to coordinate nitrogen. The situation is likely to be similar in related phases, notably in *o*′-sialon.

A method proposed [35] for calculation of shell radii for two spheres separated only by short distances was tried for this system in the refinement of the local structure around the silicon atom in Si_2N_2O. The results from this refinement, in which two shells at almost the same distance were used, are not unreasonable, but the refinement became fragile and very sensitive to starting conditions.

4. Conclusion

The EXAFS data and analysis provide support for a structural model for the β′-sialons in which silicon occurs in different environments with respect to nitrogen and oxygen, possibly with a preference for Si–N bonds. The situation is believed to be similar for *o*′-sialons. The observed differences in bond lengths are small but the strictly uniform treatment of all data sets has made it possible to compare the results for β′-sialons and Si_3N_4 and extract useful structural information.

TABLE I Bond distances in the first coordination sphere

Sample	Si–O/N (nm)	Al–O/N (nm)	Diffraction data (nm)		Reference
			Si–O/N	Al–O/N	
B1	0.169	0.177			
B2	0.168	0.176			
α-Si_3N_4	0.171		0.174		[28]
Cristobalite	0.161		0.160		[29]
Xerogel	0.161				
NaA	0.161	0.174	0.162	0.172	[30]
AlN		0.183		0.190	[31]
Anorthite		0.175		0.174	[32]
Si_2N_2O	0.161/0.170		0.161/0.172		[33]

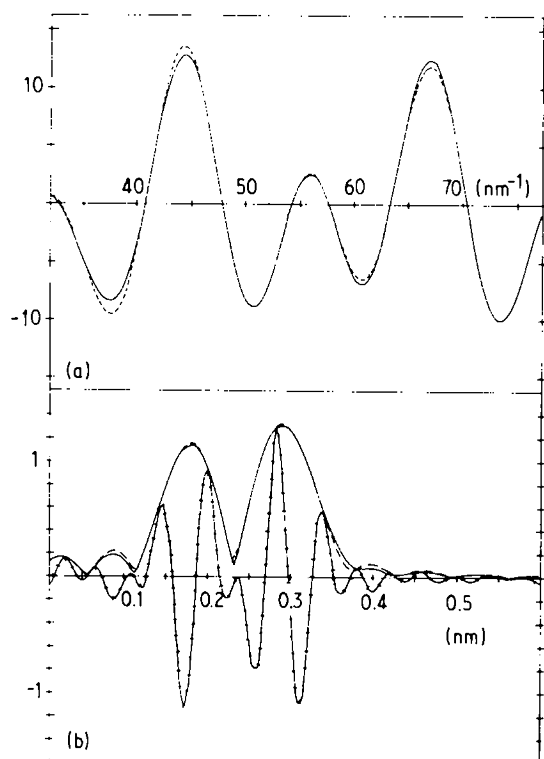

Figure 4 (a) Contribution to Al*K* edge $k^3\chi(k)$ from the first and second scales in anorthite ( ) experimental, ( ) theoretical, and (b) its radial distribution function, (·····) experimental and (– – –) theoretical, including (++++ +) the theoretical sine transform.

Acknowledgements

The assistance of the staff at SRS Daresbury at all stages of the EXAFS work is appreciated. Dr C. O'Meara is thanked for her work on the TEM. Travel grants from the Swedish Natural Science Research Council are gratefully acknowledged.

References

1. K. H. JACK, *Ceram. Civil.* **III** (1987) 259.
2. P. E. D. MORGAN, *NATO ASI Ser.* **E23** (1977) 23.
3. P.-O. OLSSON, Thesis, University of Stockholm, *Chem. Commun. Univ. Stockholm* (2) (1989).
4. K. H. JACK, *J. Mater. Sci.* **11** (1976) 1135.
5. T. EKSTRÖM, P.-O. KÄLL, M. NYGREN and P.-O. OLSSON, *ibid.* **24** (1989) 1853.
6. M. B. TRIGG and K. H. JACK, *J. Mater. Sci. Lett.* **4** (1987) 407.
7. L. GILLOT, M. COWLAM and G. E. BACON, *J. Mater. Sci.* **16** (1981) 2263.
8. F. K. VAN DIJEN, R. METSELAAR and R. B. HELMHOLDT, *J. Mater. Sci. Lett.* **6** (1987) 1101.
9. R. DUPREE, M. H. LEWIS and M. E. SMITH, *J. Appl. Crystallogr.* **21** (1988) 109.
10. R. K. HARRIS, M. J. LEACH and D. P. THOMPSON, *Chem. Mater.* **1** (1989) 336.
11. *Idem.*, *ibid.* **2** (1990) 320.
12. J. SJÖBERG, R. K. HARRIS and D. APPERLEY, *J. Mater. Chem.*, **2** (1992) 733.
13. G. ENGELHARDT and D. MICHEL, in "High Resolution Solid State NMR for Silicates and Zeolites" (Wiley, Chichester, UK, 1985) p. 36.
14. A. MOSSET and J. GALY, *Top. Cur. Chem.* **145** (1988) 1.
15. D. E. STERN, *Chem. Anal. NY* **92** (1988) 3.
16. D. E. SAYERS and B. A. BUNKER, *ibid.* **92** (1988) 211.
17. G. S. KNAPP and P. GEORGOPOULOS, *Cryst. Growth Prop. Appl.* **7** (1982) 75.
18. D. RAOUX, *Z. Phys. B Condens. Matter* **61** (1985) 397.
19. J. STÖHR, *Chem. Anal. NY* **92** (1988) 443.
20. T. EKSTRÖM and P.-O. OLSSON, *J. Amer. Ceram. Soc.* **72** (1989) 1722.
21. R. G. JONES and D. P. WOODRUFF, *Surf. Sci.* **114** (1982) 38.
22. S. M. HEALD, *Chem. Anal. NY* **92** (1988) 87.
23. S. J. GURMAN, N. BINSTED and I. ROSS, *J. Phys. C Solid State Phys.* **17** (1984) 143.
24. E. PANTOS, *Springer Ser. Chem Phys.* **27** (1983) 110.
25. E. PANTOS and G. D. FIRTH, *Technical Memorandum, Daresbury Laboratory* (1982) DL/CSE/TM21.
26. A. D. COX, in "EXAFS for Inorganic Systems", edited by C. D. Garner and S. S. Hasnain, DL/SCI/R17 (Daresbury Laboratory, 1981) pp. 51–6.
27. L. BERGSTRÖM and R. J. PUGH, *J. Amer. Ceram. Soc.* **72** (1989) 103.
28. K. KATO, I. INOUE, K. KIJIMA, I. KAWADA, H. TANAKA and T. YAMANE, *ibid.* **58** (1975) 90.
29. W. A. DOLLASE, *Z. Kristallogr.* **121** (1965) 369.
30. J. M. ADAMS, D. A. HASELDEN and A. W. HEWAT, *J. Solid State Chem.* **44** (1982) 245.
31. H. SCHULZ and K. H. THIELMANN, *Solid State Commun.* **23** (1977) 815.
32. C. J. E. KEMPSTER, H. D. MEGAW and E. W. RADOSLOVICH, *Acta Crystallogr.* **15** (1962) 1005.
33. J. SJÖBERG, G. HELGESSON and I. IDRESTEDT, *ibid.*, **C47** (1991) 2738.
34. D. RAOUX and A. M. FLANK, in "EXAFS and Near Edge Structure III", edited by K. O. Hodgson, B. Hedman and J. E. Penner-Hahn (Springer, Berlin, 1984) pp. 321–5.
35. J. B. A. D. VAN ZON, D. C. KONINGSBERGER, R. PRINS and D. E. SAYERS, *ibid.*, pp. 89–91.

*Received 9 September
and accepted 20 December 1991*